

Energy Transfer in Mechanical Alloying (*Overview*)

M. Magini and A. Iasonna

ENEA, C.R. Casaccia, Via Anguillarese, 301-00060 Roma, Italy

It is essential to understand in which way and how much energy is transferred from the milling tools to the powder in the milling process. We have attempted to quantify the energy transferred per impact and per unit of mass in a planetary mill assuming that collision is the dominant energy transfer event. Further, attrition mechanism (rolling/sliding) has been considered by evaluating the effect of filling the milling vessel. The energy transfers evaluated by the above modelization have been proved to be able to correlate the input energy and the different solid state reaction undergone by the Pd-Si system submitted to the milling action in both planetary and shaker mills. Measurements of power consumption during the milling process have been also performed and compared with those based on theoretical modelization. The fairly good agreement obtained gives a strong support to the validity of the theoretical background.

(Received October 11, 1994)

Keyword: mechanical alloying, modelization, energy transfer, power measurements

I. Introduction

Mechanical alloying (MA) is a well established technique in solid state powder processing and has already received industrial exploitation for the oxide dispersion-strengthened alloys production after the pioneer work of Benjamin⁽¹⁾. At qualitative level the phenomena occurring when milling ductile powders have been understood and consist, essentially, in a continuous process of deformation, fracture and welding as described, *e.g.*, in Ref. (2).

A deeper insight into the process would require to know how energy is transferred from the milling tools to the milled powder and in which way the energy transferred promotes network strains, atomic diffusion, temperature and pressure rises, etc. The energy transfer, of course, will depend on the kind of mill and, for the same mill, on the operative milling conditions. The final goal of a quantitative description of the process is to establish predictive capabilities so that a wanted final product can be planned as a function of the conditions of milling.

The first modelling attempts have been done in order to estimate the temperature rise during collision⁽³⁾⁽⁴⁾. By a more sophisticated model Maurice and Courtney⁽⁵⁾ tried to estimate relevant process parameters like impact time, temperature rise, powder strain and others. We have described the kinematic equations of a ball moving in a planetary mill⁽⁶⁾ and obtained an evaluation of the kinetic energy of the balls. By that approach we were able to estimate the energy transfer due to the ball impact and establish a fairly good correlation between milling conditions and end products⁽⁶⁾⁽⁷⁾.

In the previous approaches⁽⁵⁾⁽⁶⁾, collision has been considered the only energy transfer event. Over a broad range of milling operative conditions, the assumption is realistic. However, when a ball milling, whatever it is, becomes filled up with balls, attrition phenomena (sliding and rolling) play a role more important than collision

and the information coming from the models becomes inadequate.

In principle, both collision and attrition should be considered. Collision prevails when the milling device contains few milling tools as shown in Fig. 1(a): there the collision between balls and the opposite wall is the dominant energy transfer event. When the mill begins to be filled up with balls, it will approach the situation described for the classical attritor for Oxide Dispersion Strengthened Alloys production⁽²⁾, shown in Fig. 1(b), where shear stress between neighbouring balls is the dominant energy transfer event.

Recently, Le Brun *et al.*⁽⁸⁾ and McCormick *et al.*⁽⁹⁾ showed by video recordings that the movements of the balls is rather different from the one depicted in Fig. 1(a) and that sliding and rolling between balls occur even if the filling of the vial is low⁽⁹⁾. However, collisions still are operative (probably not only with the opposite wall as schematized in Fig. 1(a) but also between balls) and the collision approach, as we will show in the following, is able to give a satisfactory explanation of the experimental findings both at low level and also, with a correction factor, at high level of filling.

II. Evaluation of the Energy Transferred during the Milling Process. Construction of an "Energy Map"

As we have mentioned in the introduction the complexity of the milling process can be, conceptually, simplified in two different elemental mechanical actions by which energy is transferred from the milling tools to the milled powder: collision and attrition. The mechanism of collision prevails when the milling device contains a limited number of balls. On the contrary it is expected that the attrition mechanism prevails when the mill begins to be filled up with balls.

In a real milling process with a given mill and a given

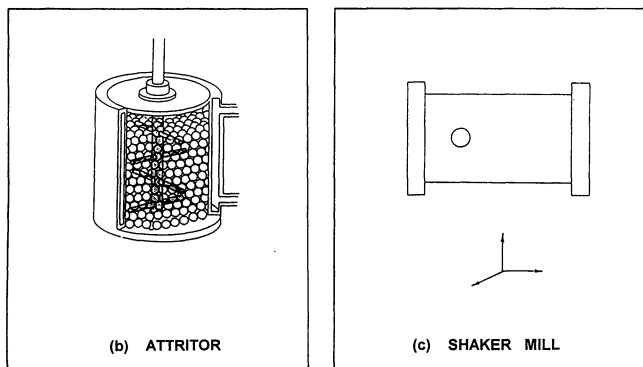
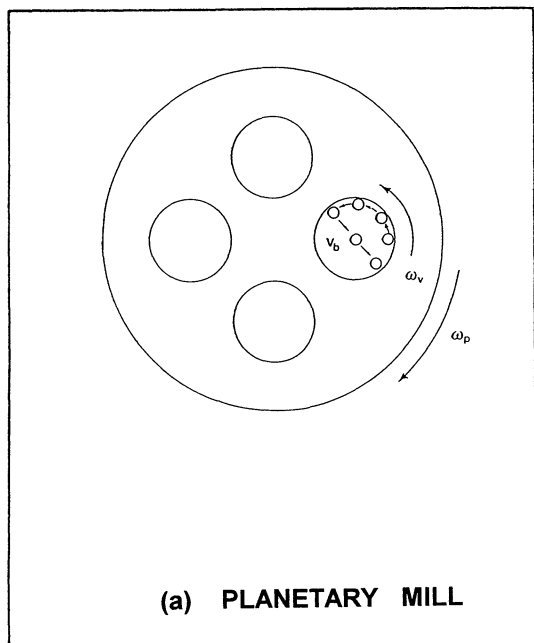


Fig. 1 (a) Scheme of the planetary ball mill. ω_p and ω_v , the angular velocities of the ball mill plate and of the vial, respectively. The trajectory of a ball is indicated. (b) Classical attritor for ODS production. (c) Scheme of a shaker mill. The device receives impulses in three directions of the space although the amplitude of the motion is prevailing in one direction.

charge the two mechanisms are certainly both operative and cannot be separated. Cinematographic video recordings⁽⁸⁾⁽⁹⁾ shows that even when collision is largely dominant, tumbling of the balls occurs and both sliding and rolling contribute to the global process of energy transfer. However, it is possible to set up experiments in which it is expected that one of the two mechanisms is dominant so that energy transfer can be analysed in the wanted conditions.

1. Collision regime

Collision has been assumed to be the energy transfer event in the first hints attempted to get information on the MA process⁽³⁾⁽⁴⁾. Subsequent modelizations⁽⁵⁾⁽⁶⁾ were also based on collision although attention was drawn on the fact that when the mill begins to be filled up with balls, a "filling factor" had to be taken into proper con-

sideration⁽⁶⁾.

Nevertheless, when the filling charge of the mill is low, as next described, the collision can be assumed to be the prevailing energy transfer source and this assumption underlies this section. If the collision is the basic event by which, during milling, power is transferred from the mill to the powder, then the main problems to solve are:

- (i) evaluation of the kinetic energy of the ball: $(1/2)mv^2$;
- (ii) evaluation of the fraction of the kinetic energy given to the powder;
- (iii) evaluation of the quantity of material entrapped in the collision event.

(1) Kinetic energy of a ball in a planetary mill

Recently, McCormick *et al.*⁽⁹⁾ suggested an improvement of the basic model described in Ref. (6) considering a "slip factor" that takes into account the sliding phenomena between balls and wall. By this factor the calculated trajectory of the moving balls becomes more realistic and similar to that video recorded⁽⁸⁾⁽⁹⁾.

Nevertheless, the collision still remains the primary energy transfer event and the main conclusions previously drawn are still valid. The summary of the previous kinematic equations⁽⁶⁾ with further graphical evaluations⁽¹⁰⁾, allow to derive the *relative impact velocity*, v_b , of a ball impacting on the wall:

$$v_b = K_b \omega_p R_p \quad (1)$$

where R_p is the radius of the plate of the mill. K_b depends on the geometry of the mill and, for the planetary mill here discussed, is worth ~ 1.06 for a point ball and ~ 0.90 for a ball of diameter of 10 mm⁽¹⁰⁾.

For each measurable rotation speed of the supporting plate, ω_p , the relative impact velocity is known from eq. (1). The kinetic energy involved in the collision is then given by $(1/2)m_b v_b^2$, being m_b the mass of the ball. The energy *released* in each collision is given by:

$$\Delta E = K_a \frac{1}{2} m_b v_b^2 \quad (2)$$

where K_a is a coefficient depending on the elasticity of the collision. For perfect elastic collisions the energy release is null ($K_a=0$) and is total ($K_a=1$) for perfect inelastic collisions. Combining eqs. (1) and (2) we have:

$$\Delta E = K_c m_b \omega_p^2 R_p^2 \quad (3)$$

where K_c includes the constant values of eqs. (1) and (2).

Figure 2 is the graphical representation of eq. (3) and gives the energy released per hit as a function of the operative milling conditions affecting the energy transfer, namely: the rotation speed of the mill and the mass of the ball (i.e. the diameter, like in Fig. 2, for a given material). The energy transfer greatly depends on the elasticity of the collision and this point is dealt with in the next section.

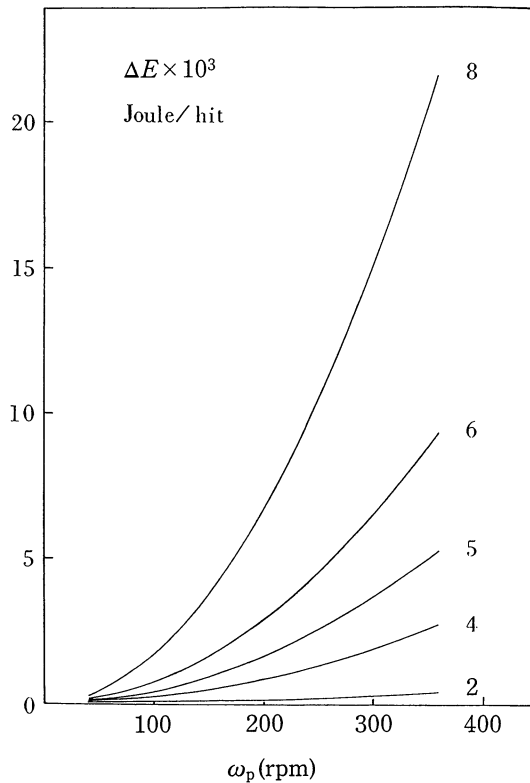


Fig. 2 Energy dissipated per hit plotted versus the rotation speed of the planetary mill (in rounds per minute) when using stainless steel balls. The number near each curve is the ball diameter in millimetres.

(2) "Free fall" experiment-Evaluation of the kinetic energy transferred to the powder

The family of curves represented in Fig. 2 have been drawn for $K_a=1$ (perfect inelastic collision) and give therefore the maximum of energy released in a collision event. If the collision is not totally inelastic ($0 < K_a < 1$), the curves will be lowered down accordingly. Whatever be the real situation in a real milling process, the energy release depicted in Fig. 2 concerns the "system" involved in the collision event, that is the powder trapped, the impacting ball and the hited region wall. Which fraction of the total energy involved is really given to the powder under processing? The analysis of the collision event shown in the following answer to the question.

We have simplified the collision event occurring in a mill by letting balls of different diameter fall with gravity on a large plate of the same material. The heights of launches were such that the impacting velocities reproduced those occurring in a mill. Firstly, rebounds of bare balls have been recorded by a videotape camera and the rebound yields obtained by the relation:

$$\eta = h' / h \quad (4)$$

where $\eta = 1 - K_a$ and h' and h are the heights of the launch and of the rebound respectively. The energy involved in the collision is given by:

$$E_o = m_b g h = \frac{1}{2} m_b v_b^2 \quad (5)$$

and the energy after the jump given by:

$$E'_o = m_b g h' = \eta E_o \quad (6)$$

The same experiments have been carried out with balls charged with powder taken out at different times during the milling process and the η_i , rebound yield with coated ball, measured. Typical rebound yields for both bare and coated balls are shown in Fig. 3.

The energy *released* during the collision, is simply given by the total energy involved in the impact, E_o , minus the energy restituted as potential energy $m_b g h'$, that is:

$$\Delta E = E_o - E'_o = E_o(1 - \eta) \quad (7)$$

The ΔE values are shown in Fig. 4. Table 1 gives representative values of the free fall experiments with bare balls.

It is shown in Fig. 4 that in the early stages of milling (see the points at 1 hour) the energy dissipation per hit approaches the boundary limit of the total dissipation energy (upper straight line of the figure) which is realized when the ball does not rebound at all.

The two limiting curves of Fig. 4 (bare balls and total dissipation) indicate that, for any given E_o , most of the kinetic energy dissipated per hit goes to the powder. Moreover, it is obvious that when the ball is coated the energy dissipated into the ball is much lower than that shown in Fig. 4 for bare balls.

The previous qualitative observation is better quantified by the following simplified treatment. During the

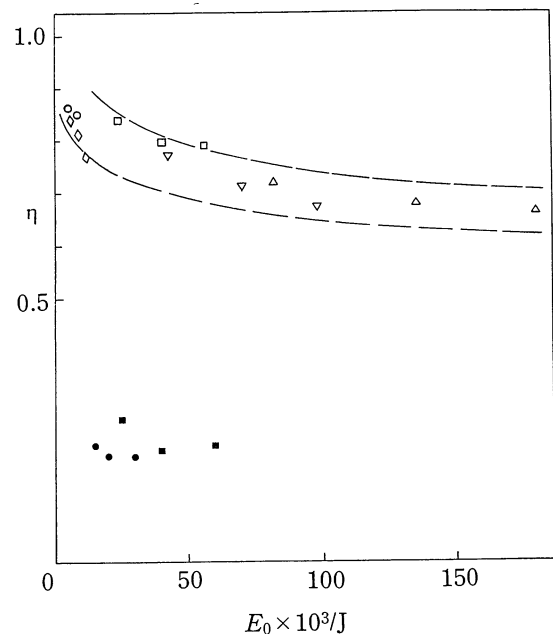


Fig. 3 Rebound yield of bare and coated balls, η , plotted as a function of the kinetic energy of the balls at the moment of the impact, E_o . Open symbols refer to bare ball of diameter: (\circ) 5 mm; (\diamond) 6 mm; (\square) 10 mm; (∇) 12 mm and (\triangle) 15 mm. Full symbols refer to coated balls (1 hour of milling) of diameter: (\bullet) 8 mm and (\blacksquare) 10 mm. A TiAl powder (Ti:Al=1:1) has been used to coat the balls in these experiments as well as for the experiments of Fig. 4.

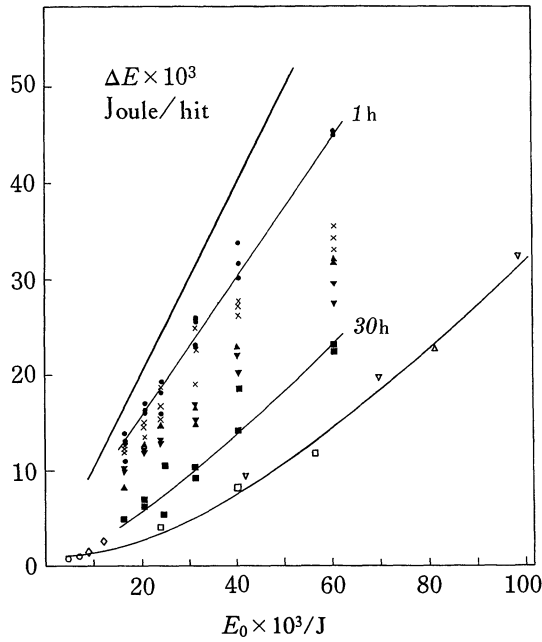


Fig. 4 Energy dissipation during impact, ΔE , plotted versus E_0 (see Fig. 3). The open symbols refer to the bare balls of Fig. 3. The full symbols refer to experiments with balls charged of powder at different milling times \bullet , \times , \blacktriangle , \blacktriangledown and \blacksquare = 1, 2, 5, 15 and 30 h of milling. At each milling time one symbol has been used for each of the ball used in the free fall experiments. The upper straight line represents a total dissipation energy curve (see text). The lowest curve, as well as those at 1 and 30 h of milling, have been drawn through the experimental points for clarity.

impact time we can conceive that the total energy E_0 is partitioned between the ball and the powder:

$$E_0 = E_b + E_p \quad (8)$$

where the term E_b takes into account also the contribu-

tion coming from the plate. After the jump the energy restituted may be expressed as

$$\eta_t E_0 = \eta_b E_b + \eta_p E_p \quad (9)$$

where η_t and η_b have been defined and measured and η_p is the elastic yield of the powder. Since, it is reasonable to assume, for plastic metals, that $\eta_p \approx 0$, it follows that

$$E_b = E_0 \eta_t / \eta_b \quad (10)$$

and therefore from eq. (8)

$$E_p = E_0 (1 - \eta_t / \eta_b) \quad (11)$$

from which E_p can be estimated. From a starting guessed E_b value, η_b is obtained through the relation (η_b ; E_0) of Fig. 3 and hence a first evaluation of E_p can be done. The procedure can be iterated, through eqs. (8) and (11), up to a constant E_p value. Exemplification values of such evaluations are reported on Table 2. It can be seen from the table that with respect to the total energy dissipated (column 5), the energy dissipated onto the powder, E_p (column 6), amounts practically to the total in the early stage of milling. If we consider that our experiments with coated balls have been carried out using a free surface plate (i.e. the measured η_t values are greater than in the real milling process where the vial walls, like the balls, are covered with a thin powder layer), it is highly reasonable to assume that in the early milling stages the kinetic energy is totally dissipated and this energy is totally given to the powder.

(3) Quantity of material trapped in a collision event

The analysis of the collision previously described allow to assume that the curves of Fig. 2 really represent the energy given to the powder in a real milling process, at least as long as the collision can be considered to be inelastic.

A further step can be accomplished by evaluating the

Table 1 Parameters of the free fall experiments with bare balls. d_b and m_b diameters and masses of balls; h , the heights of launches; V_0 and E_0 the velocities and the energies at the impact; η_b the rebound yield and ΔE_b the energy dissipated in the impact.

d_b 10^{-3} [m]	m_b 10^{-3} [kg]	h [m]	V_0 [m/s]	E_0 10^{-3} [J]	η_b	ΔE_b 10^{-3} [J]
5	0.514	1.00	4.43	5.05	0.87	0.7
		1.40	5.24	7.07	0.85	0.1
6	0.889	0.60	3.43	5.23	0.84	0.8
		1.00	4.43	8.72	0.81	1.7
		1.40	5.24	12.21	0.77	2.8
10	4.085	0.60	3.43	24.03	0.84	3.9
		1.00	4.43	40.06	0.80	8.0
		1.40	5.24	56.08	0.79	11.8
12	7.116	0.60	3.43	41.88	0.77	9.5
		1.00	4.43	69.79	0.71	20.0
		1.40	5.24	97.73	0.67	32.5
15	13.899	0.60	3.43	81.80	0.72	22.6
		1.00	4.43	136.30	0.68	43.6
		1.40	5.24	190.90	0.67	63.0

Table 2 Fraction of energy given to the powder in free fall experiments with coated balls of 10 mm launched from 100 cm height at different milling times. The meaning of column headings are the same as in Table 1. A, B, C identify different balls for the same experiment.

Time [h]	Ball	η_t	$\langle \eta_t \rangle$	ΔE_t 10^{-3} [J]	E_p 10^{-3} [J]	$(E_p / \Delta E_t) 100$
1	A	0.16				
	B	0.26	0.21	31.6	30	95
	C	0.22				
2	A	0.35				
	B	0.32	0.33	26.8	24	90
	C	0.32				
5	A	0.45	0.43	21.2	16	78
	B	0.41				
15	A	0.43	0.42	22.8	19	82
	B	0.41				
30	A	0.64	0.59	16.4	9	55
	B	0.53				

powder entrapped during the collision. We know from the experiments that in the early stages of milling most of the powder adheres to the surface of the balls and the vial walls. It should not be far from reality to assume that the powder trapped in between during a collision is, at the minimum, the one adhering to the surfaces. Measuring the weight of the balls as a function of the milling time, we can estimate the surface density, σ , of the covering powder.

The area of impact is a circular area whose radius is given, in the Hertzian collision approximation⁽¹¹⁾, by

$$R_h = [\delta(R_1 R_2)/(R_1 + R_2)]^{0.5} \quad (12)$$

or, considering R_2 (the radius of the vial) $\gg R_1$ (radius of the ball = $d_b/2$),

$$R_h = \delta^{0.5} R_1^{0.5} \quad (13)$$

with $\delta = \delta_1 + \delta_2$ the sum of compression of the colliding tools as illustrated in Fig. 5. At the maximum of compression $R_{h,max}$ takes the following form for colliding media of the same material:

$$R_{h,max} = 1.1076 v_b^{0.4} m_b^{0.2} R_1^{0.4} / E^{0.2} \quad (14)$$

E being the Young modulus of the material. Once known the maximum impact radius, the maximum impact surface, S_{max} is obtained. The maximum quantity of trapped material is given by:

$$Q_{max} = 2\sigma\pi R_{h,max}^2 \quad (15)$$

where the factor 2 assumes that twice the surface density (ball and vial surface) must be considered. The final equation expressing the energy transferred per unit of mass is obtained dividing eq. (3) by eq. (15):

$$\Delta E/Q_{max} = [7.66 \times 10^{-2} R_p^{1.2} \rho^{0.6} E^{0.4}] d_b \omega_p^{1.2} / \sigma \quad (16)$$

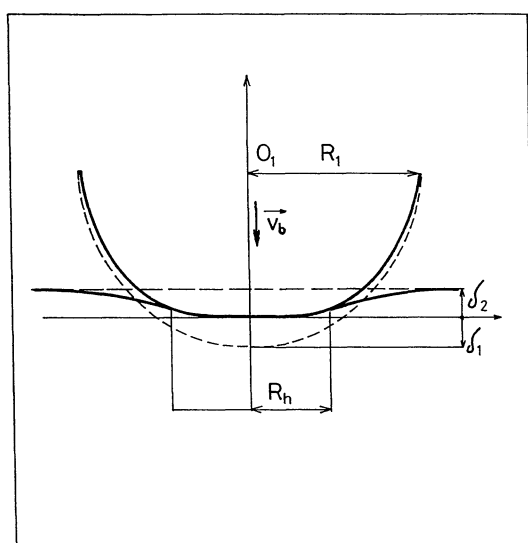


Fig. 5 Scheme of the collision event of a ball of radius R_1 and relative velocity v_b against a flat surface. Dashed and solid lines represent the non deformed and deformed bodies. R_h is the radius of the contact surface; δ_1 and δ_2 are the displacements along the impact axis.

where ρ is the ball material density. Expressing all the variables in international units, for our planetary mill ($R_p = 0.122$ m) and considering stainless steel tools ($\rho = 7.64 \times 10^3$ kg/m³ and $E = 2.1 \times 10^{11}$ N/m²) the value enclosed in squares parenthesis becomes 4.43×10^4 and $\Delta E/Q_{max}$ will be expressed in J/kg.

Equation (16) is a useful tool able to rationalize the experiments we have carried out properly varying d_b or ω_p .

(4) Milling experiment with the Pd-Si system

The Pd₈₀Si₂₀ system possesses a peculiarity that we have not been able to detect at the same level of clarity in any other system up to now investigated. Submitted to the milling process (that must be controlled with respect to oxygen contamination⁽¹²⁾), the system clearly follows two different and distinct pathways depending on the milling conditions. The behaviour is summarized in Figs. 6 and 7. Figure 6 shows that, in given milling conditions, the system gradually evolves towards the formation of an amorphous phase. Figure 7 shows that, in other conditions, Pd and Si immediately react to form the intermetallic compound Pd₃Si (in mixture with minor fractions of other intermetallic compounds). The formation of the intermetallic is accomplished in the very early milling stages. The formation of the amorphous phase is gradual but, again, the path is chosen at once since the broadening of the Pd lines, instead of the appearance of the intermetallic lines, has always proved to be indicative of the amorphous pathway.

The Pd-Si system seemed therefore useful in order to test the modelizations previously described i.e. the final eq. (16). A large number of experiments have been carried out by a planetary mill (Model "Pulverisette 5" from FRITSCH) using different operative milling conditions. Most of them have been summarized in Table 3. The σ value appearing in eq. (16) has been estimated and is of the order of 0.3 mg/mm² in the early stages of mill-

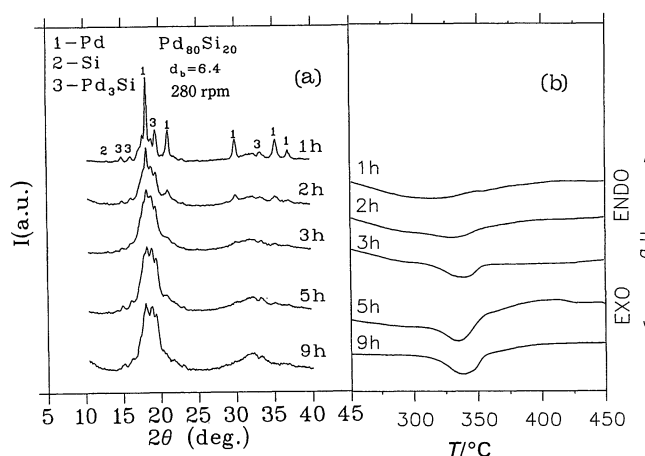


Fig. 6 Intermetallic pathway. X-ray patterns (a) and DSC traces (b) as a function of the milling times for the Pd₈₀Si₂₀ composition with the indicated milling conditions (d_b = ball diameter, rpm = rotation speed run per minute). The X-ray pattern at 1 h of milling clearly indicates the formation of the intermetallic Pd₃Si compound. The thermograms do not indicate a glass-crystalline transition.

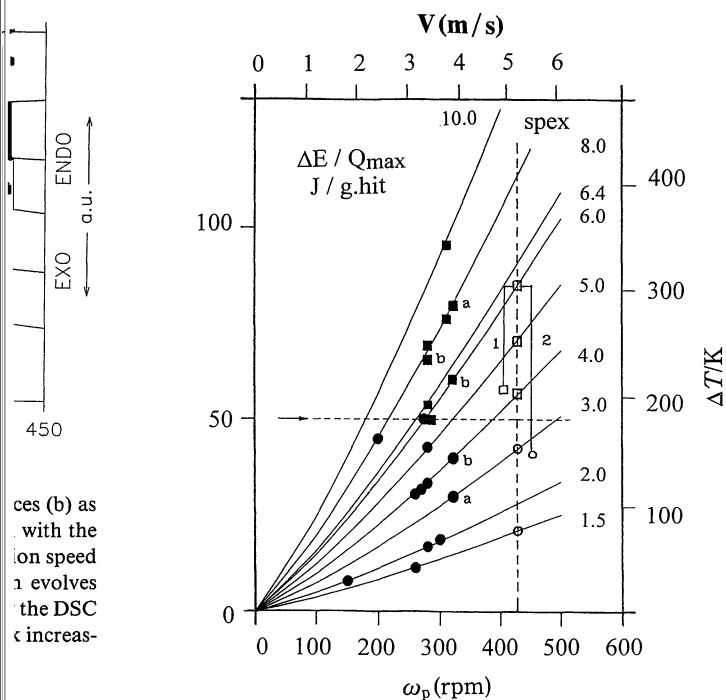


Fig. 8 The continuous lines represent the energy transferred per hit and per unit of mass as a function of the rotation speed of the planetary mill in rpm (rounds per minute) for each ball diameter used (given in mm near each curve) and assuming $\sigma=0.3 \text{ mg/mm}^2$ (see text). Each full and open symbols represent experiments carried out on planetary and shaker mill respectively. Squares and circles identify the intermetallic or amorphous pathway respectively. The horizontal upper axis is the velocity of the ball in m/s (eq. (1)); while the right hand-side vertical axis is the average instantaneous temperature rise (see text). The vertical dashed line and the open symbols on it represent the experiments carried out on a shaker device all the experiments have been carried out on the $\text{Pd}_{80}\text{Si}_{20}$ composition with exception of (a) = $\text{Pd}_{86.5}\text{Si}_{13.5}$ and (b) = $\text{Pd}_{83}\text{Si}_{17}$. The lines marked by (1) and (2) indicate two attrition experiments (see text).

ould be constant when systematic and

on Fig. clearly shows above phases is given omitted option tic tem- fic heat e work ion and $10^{-5} \text{ s}^{(5)}$ probably y trans- tic tem- perature s about valls by ig time hose of h atten- ine that terature he reac- ibution

the tly used

mills around the world belongs to planetary or shaker types, it would be desirable then to establish usable correlations between them in order to make possible cross comparison of different experiments. In fact, most of the experimental results appeared in the last years are not comparable because the conditions of energy transfer are often not known even for the same apparatus, and at most, only qualitative comparisons have been done. We carried out, therefore, a number of experiments with a shaker device (model "8000" from SPEX) and used the map of Fig. 8 to correlate the two different mills.

Considering that the shaker mill schematized in Fig. 1(c) is subject to impulses in the three directions of the space, it is hard or impossible at all to derive the kinematic equations like it has been done for a planetary mill⁽⁶⁾. We used, therefore, the map of Fig. 8 to infer, in an indirect way, the relative impact velocities occurring in such a device. To do that we have experimentally looked for the threshold value when milling with the shaker mill using different ball diameters. Since the vibration frequency is fixed the situation is like the one of the planetary mill at fixed ω_p and the threshold should appear at a given ball diameter.

Table 3 Conditions of milling adopted in experiments with planetary (upper part) and shaker (lower part) mills. rpm, and d_b are the main variable of the milling conditions (see text). PW is the total weight of powder used and RPB the ratio balls/powder weights. The last column indicates the solid state reaction path chosen by the Pd-Si system: I=intermetallic; A=amorphous path.

rpm [min ⁻¹]	d_b [mm]	PW [g]	RPB	Pathway
310	10	10	5	I
310	8	10	5	I
280	8	10	5	I
200	8	10	5	A
280	6.4	10	5	I
280	6	10	5	I
280	6	10	5	A
280	5	10	5	A
280	4	10	5	A
280	4	15	5	A
270	4	10	5	A
260	4	10	5	A
300	2	5	5	A
280	2	10	5	A
150	2	5	5	A
260	1.5	2.2	5	A
320 ^(a)	8	5	5	I
320 ^(a)	3	5	5	A
320 ^(b)	6	5	5	I
320 ^(b)	4	5	5	A
S	10 ^(d)	4	10	I
S	6	2	10	I
S ^(c)	6	5	28	I
S ^(c)	6	8	20	A
S	4	2	10	I
S	3	2	10	A
S	1.5	3	10	A
S	1.5	1	5	A

^(a) Pd_{86.5}Si_{13.5}

^(b) Pd₈₃Si₁₇

^(c) high level of filling (see text)

^(d) WC balls

The experiments carried out are given in the lower part of Table 3. All of them but two (discussed in the next section) fulfils the requirement of a low level of filling in order to satisfy the collision regime. A clear threshold value has been detected between the diameters of 3 and 4 mm. Entering the map of Fig. 8, the relative impact velocity of the SPEX mill should lie between 5 and 6 m/s. The value is in fairly good agreement with those of 3.9 reported by Maurice and Courtney⁽⁵⁾, and 6 m/s given by Davis *et al.*⁽⁴⁾.

2. Attrition regime

From a given filling of the vial on, reciprocal hindering of the ball begins, and one must expect that the modelization based on collision becomes inadequate to describe the energy transfer.

In the condition of high filling, attrition phenomena are no longer negligible and collisions themselves become less effective because, probably, the mean free path and the relative impact velocity are lowered. We will call this situation as the "attrition regime" although both attrition and collision are probably operative. What we expect is that the reciprocal hindering leads, ultimately, to

a *less efficient* energy transfer.

In order to quantitatively evaluate the effect of the filling factor we have done the following. Let us assume that in the attrition regime the energy transfer is still given by eq. (2) but damped down by a filling factor ϕ_b less than one, i.e.:

$$\Delta E^* = \phi_b \Delta E \quad (17)$$

In an ideal experiment the total power consumption, P , will be proportional to the energy transfer per hit, to the frequency of the hits and to the number of balls, N_b , through an expression of the type:

$$P = K' N_b f_b \Delta E_b^* = K' N_b f_b \phi_b \Delta E \quad (18)$$

since the hit frequency f_b is proportional to the rotation speed ω_p ⁽⁶⁾ and ΔE can be expressed through eq. (3) it follows that:

$$P = K_\phi \phi_b N_b m_b \omega_p^3 R_p^2 \quad (19)$$

Remembering that when $N_b \rightarrow 0$, $\phi_b \rightarrow 1$ for any ball diameter, the factor ϕ_b can be obtained by:

$$\phi_b = [(P/\omega_p^3 N_b m_b)] / [(P/\omega_p^3 N_b m_b)]_{N_b \rightarrow 0} \quad (20)$$

Equation (20) allows the evaluation of the filling factor ϕ_b , provided that suitable power measurements consumption can be done. As we will see in Section III this kind of measurements have been set up and, for the present question, power measurements have been carried out in the planetary mill by charging 2 or 4 vials with increasing amount of balls of different diameters and by measuring the power consumption as a function of the rotation speed ω_p . The results of such measurements have been introduced in eq. (20) and the ϕ_b values so far obtained have been plotted in Fig. 9 as a function of the filling of the vial n_v defined as:

$$n_v = N_b / N_{tot} \quad (21)$$

where N_b and N_{tot} are the number of balls used in the experiments and the total number of balls needed to completely fill up the vial.

Figure 9 predicts that the energy transfer should be reduced by increasing n_v and therefore we should be able to cross the threshold of Fig. 8 by simply increasing the filling of the vial keeping constant the other milling conditions.

We have milled the Pd₈₀Si₂₀ composition with three different fillings of balls with $d_b=6$ mm (see Table 3 lower part). The three fillings have been indicated in Fig. 9 and the end products shown in Fig. 10. At low filling ($n_v \leq 0.1$) the system follows the intermetallic route (Fig. 10(a)). At higher level of filling ($n_v \cong 0.5$) the energy transfer is damped down by a $\phi_b \sim 0.75$ that is not enough to cross the threshold intermetallic/amorphous as shown in Fig. 8. At still higher filling ($n_v \cong 0.7$ and $\phi_b \sim 0.5$) the energy map predicts that the threshold can be crossed and now the amorphous route is followed (see Fig. 10(b)).

3. Comments on the "energy map"

The principles exposed in the present work for the Pd-

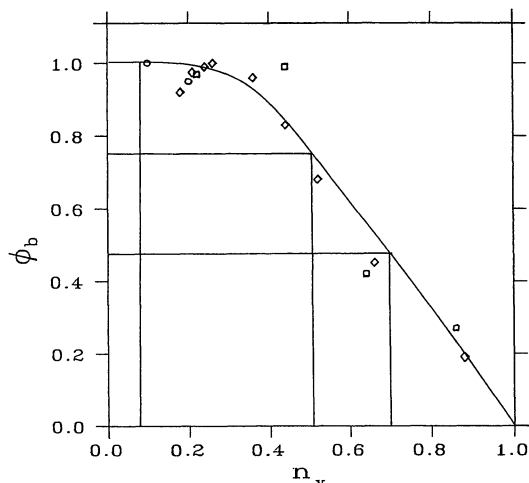


Fig. 9 Experimental evaluation of the filling factor, ϕ_b , versus the filling of the vial n_v with different ball diameters (\circ , \diamond , \square for 6, 10, 15 mm, respectively). Three different experiments have been indicated for $n_v < 0.1$ ($\phi_b \sim 1$); $n_v \cong 0.5$ ($\phi_b \sim 0.75$) and $n_v \cong 0.7$ ($\phi_b \sim 0.5$) (see text).

Si system, are valid, in our opinion, for any other system prone to undergo different solid state reactions and we feel, therefore, that some fundamentals have been put in order to correlate energy input and results of the milling action.

However, it is opportune to analyse the *sources of errors* underlying our arguments or, in other words, to discuss the reliability of our approach.

The energy released per hit is given by eq. (2), which, in turn, depends on the evaluation of the relative impact velocity through eq. (1). Our estimated velocities do not differ from those appeared in Refs. (4) and (5) and, above all, they would eventually affect the flow of argument by a *systematic error*.

The same is true for the evaluation of the impact area derived from an Hertzian elastic collision while in the real case, just in the early milling stages, the collision is inelastic. This fact surely affects the evaluated impact area by approximately 10–20% but, again, in a *systematic way* so that the energy map will still maintain its validity.

The more crucial point, in our opinion, concerns the quantity of trapped material assumed to be the one adhering to the surfaces, i.e. the evaluation of the real surface density σ . The surface density values have been obtained from direct weight measurements. The average measured value of 0.3 mg/mm^2 should represent a minimum value of the real quantity of material trapped since some powder, not adhering to the surface, can also be involved. Anyway, while it is reasonable to assume that the powder trapped in the collision is, at least, the one adhering to the surfaces, the experimental values measured may actually vary by a factor of 2⁽¹³⁾. The σ parameter, therefore, is probably the major factor of uncertainty in the absolute evaluation of the energy transferred per unit of mass.

Further, after having analysed the sources of error, we

have to add that in the previous considerations we always refer to values related to a collision, that is values averaged over the interval time of the collision event ($\sim 10^{-5} \text{ s}$). The powder trapped at the centre of the colliding area at the beginning of the impact will have a completely different history from the one at the borders of the same area reached at the end of the compression time. From this point of view the local instantaneous energy transfer *during the collision time* may greatly differ from the “instantaneous average” values here considered and only an analysis of a single collision on a nanosecond scale could provide a more accurate description of what is really occurring.

Nevertheless, keeping all the above considerations in mind, all the experiments performed fit quite well on the map drawn with $\sigma = 0.3 \text{ mg/mm}^2$. A clear threshold value merges and the prediction capability as been tested in several ways like milling with large balls ($d_b = 8$) but at low ω_p (200 rpm) performing the attrition regime experiments (Fig. 10) and criomilling experiments⁽¹³⁾. Only experiments carried out near the threshold value gave not unambiguous results like the ones carried out at 280 rpm with ball diameter of 6 mm.

Finally, we want to stress a crucial point. If all the assumptions of the model, expressed through eqs. (1) to (16), were wrong, let us say, of an order of magnitude, the errors would be systematic and therefore a usable final map explaining the experiments could be anyway set-up. In that case, of course, the values of y axis (i.e. the energy transferred per unit of mass in a collision event) would merely be *relative* values. They should have nothing to

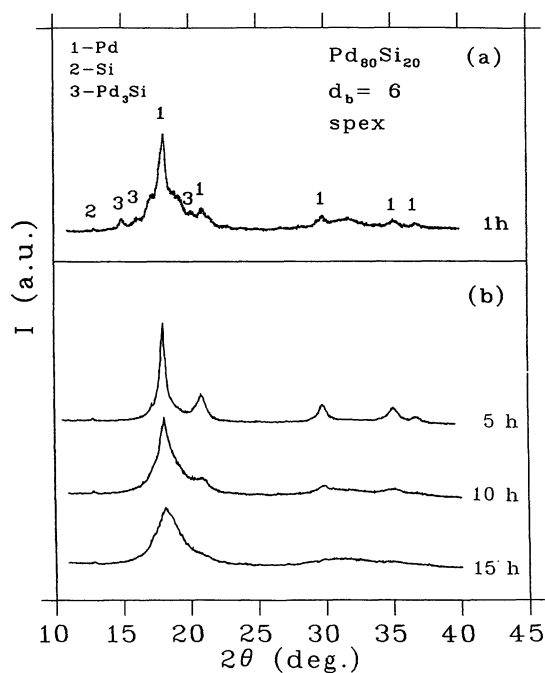


Fig. 10 Experiments carried out with the shaker device at different level of filling n_v indicated in Fig. 9. Low ($n_v \leq 0.1$) and intermediate ($n_v \cong 0.5$) fillings follow the path indicated in (a). Large filling ($n_v \cong 0.7$) follow the path indicated in (b) (see text).

do, therefore, with the *absolute* values of the energy involved in the real milling process provided that some conceivable experiments could be set up in order to infer them.

The experiments described in the next section show that this is not the case and that experiments and theory agree fairly well.

III. Measurements of Power Consumption during Milling

The energy transfer occurring during the collision event can be evaluated by eq. (2) and is of the order of 10^{-2} J/hit. The question we want to answer is the following: provided that the *order of magnitude* of the microscopic event is correct, it should be revealed at macroscopic level. Or, in other words, which kind of measurements we must conceive to confirm at experimental level the energy involved predicted by the model? We have verified that very simple measurements of electrical power absorption were highly convenient to directly support the goodness of the theory.

1. Electrical power absorption measurements

In the milling process, the energy *spent* in collisions and/or attrition derives from the movements of the milling tools: i.e. from the power given by the electrical motor. Therefore it should be possible to reveal some *absorption power difference* when milling with empty or filled vials.

Further, the free fall experiments reported on Fig. 4, clearly indicate that energy released in each collision event is little when the balls rebound elastically ($K_a \rightarrow 0$) and it is much greater when the collision is inelastic in presence of powder ($K_a \rightarrow 1$). In both cases the energy spent in the collision event is a fraction of the initial potential energy and this fraction can be measured by the experiment itself.

Again, in experiments carried out in a mill in exactly the same configuration with only highly different condition of elasticity, absorption power difference should be revealed.

We have verified the previous points by measuring by a power meter the energy absorbed by the planetary mill charged with two stainless steel empty vials. The vials have been later filled with a given number of soft stainless steel balls and, in a third experiment, with the same number of tungsten carbide balls. The three sets of data are reported in Fig. 11(a) and they show that:

- (i) there is an appreciable difference between absorption with filled or empty vials;
- (ii) there is an appreciable difference with the different elastic behaviour.

The second point is better enhanced in Fig. 11(b) where the *net power differences* between filled and empty vials are reported. We want to stress the significant analogy existing between Figs. 4 and 11(b). The energy spent in elastic collision is little and can be measured by the rebounds of bare balls or by the power absorption of tungsten carbide balls. When the collision becomes inelastic either because of the powder (free fall experiment) or because of the material (soft stainless steel in the power absorption) the energy spent in collision increases and has been registered accordingly in the two different experimental set up.

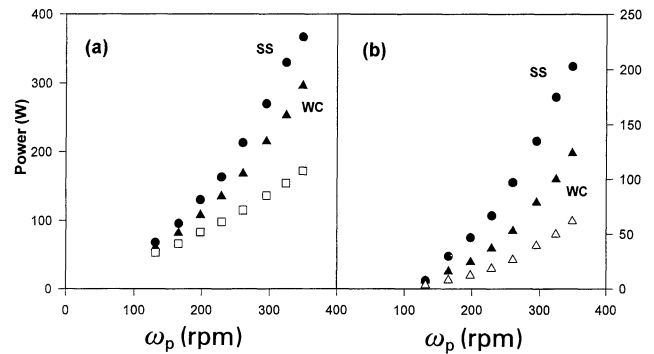


Fig. 11 (a) Electrical power absorption versus the rotation speed measured with two 250 cc vials charged with 99 stainless steel (SS) or tungsten carbide (WC) balls of 10 mm of diameter. Open squares give the absorption from the same vials empty. (b) net power differences between the absorption from charged or empty vials shown in (a): Open triangles shows the absorption from tungsten carbide balls normalized to the same weight of the stainless steel balls.

gsten carbide balls. When the collision becomes inelastic either because of the powder (free fall experiment) or because of the material (soft stainless steel in the power absorption) the energy spent in collision increases and has been registered accordingly in the two different experimental set up.

For what concerns the power absorption, the net power difference should really contain all the information concerning the sum of the microscopic events occurring during the milling process.

Once verified the feasibility of electrical power measurements we set up two experiments with powder to ensure a K_a near to one. In a first experiment two vials of 250 cm³ have been charged each with 99 balls of 10 mm diameter ($m_b=4.08$ g) and 40 g of Fe-Zr powder (Fe:Zr=1:1) already milled for three hours. The power measurements are shown by the upper points (full squares) of Fig. 12 together with the results from empty vials.

In a second experiment the two vials have been charged each with 70 balls of 8 mm ($m_b=2.10$ g) and 13 balls of 10 mm and 20 g of Ti-Al powder (Ti:Al=1:1) already milled for 5 hours. The results are given in Fig. 13. The mixture of balls of 8 and 10 mm has been hereafter considered by the asterisk 8*.

The absorption differences between charged and empty vials are shown by full triangles in Figs. 12 and 13. We notice that this net power differences, for what we know from the free fall experiments, is almost totally given to the powder. The observation, however, is not essential for the flow of arguments described below; here we wanted to outline that we have carried out experiments in presence of powder where the condition of inelastic collision is largely verified.

2. Comparison with power calculated through the model

Equation (2) gives the energy transferred during a single collision event when the collision is inelastic and kinetic

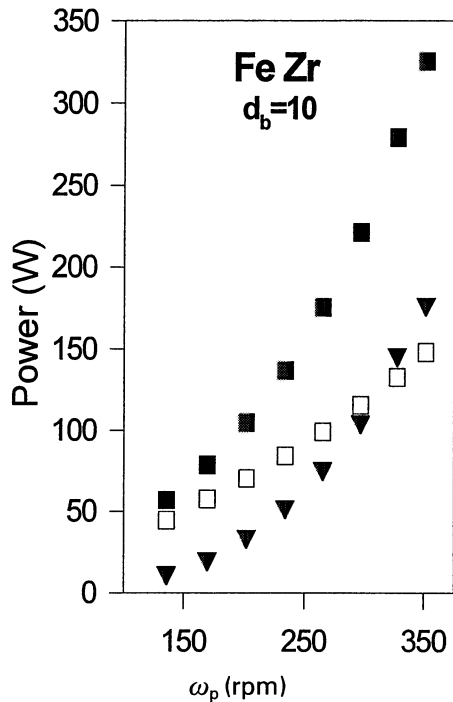


Fig. 12 Electrical power absorption versus the rotation speed for the Fe-Zr experiment. Full and open squares give the absorption of charged and empty vials respectively. Full triangles give the power differences.

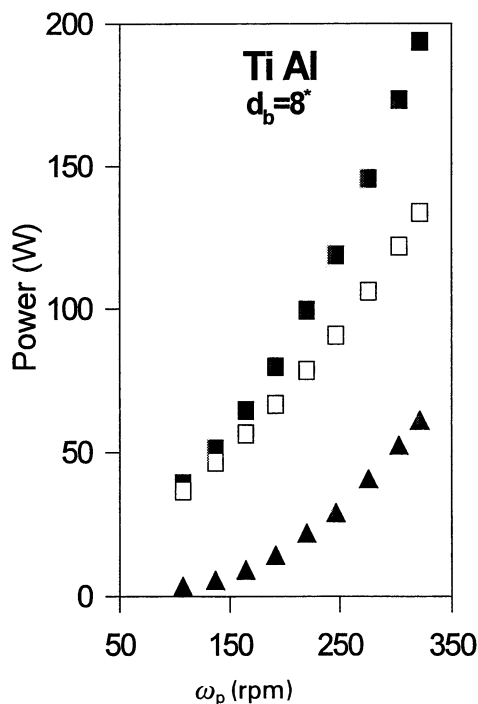


Fig. 13 The same meaning of Fig. 12 for the Ti-Al experiment.

energy is almost totally spent in collision events. The energy of a single event *multiplied by the number of events in the unity of time*, i.e. by the frequency of the hits, should give the power absorption.

The collision frequency for a single ball has been evaluated by a relation of the type:

$$\psi = K(\omega_p - \omega_v) \quad (22)$$

with ω_p in rounds per second, and ω_v , vial rotation speed, equal to $-1.25\omega_p$ ⁽⁶⁾. The K value depends on the ball diameter and has been evaluated to be of the order of 1.5 for ball diameter of 8–10 mm⁽¹⁰⁾.

Since the filling of vials in the two experiments considered is not so high, the reciprocal hindering of N_b balls is negligible in first approximation so that the total frequency collision is given by:

$$\psi_t = \psi N_b = 3.375 \omega_p N_b \quad (23)$$

and the calculated power consumption given by:

$$P_{\text{calc}} = \Delta E \psi_t \quad (24)$$

Fig. 14 shows in a straightforward way that the power consumption estimated through the model is the same as the one measured experimentally.

3. Criticism on the goodness of the theory and experiments comparison

Our aim was only to demonstrate that the *order of magnitude* of what was predicted by the model could be verified by some experimental measurements. Figure 14 actually shows a quasi-perfect coincidence between theory and experiment. This is more than satisfactory, of course, and the result cannot be changed by an order of magnitude even considering all the critical points recalled in the following. From the experimental point of view the power measurements can be affected by the real value, under operating conditions, of the electrical yield (we assumed the 80% furnished by the house). In perspective we are planning direct measurements of the applied couple⁽¹⁰⁾.

From the theoretical point of view, two factors are critics:

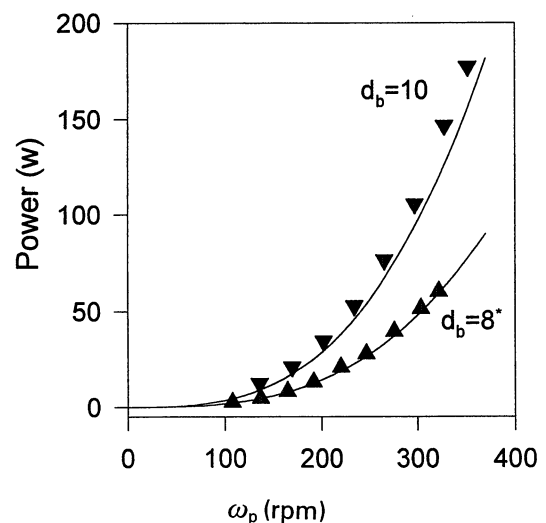


Fig. 14 Experimental (full triangles) and calculated (full lines) power absorption for the Fe-Zr ($d_b=10$) and the Ti-Al ($d_b=8^*$) experiments.

Table 4 Frequencies of the collisions as a function of the rotation speed in a planetary mill "Pulverisette 5".

ω (rpm)	ψ (s ⁻¹) (this work)	ψ (s ⁻¹) (after Gaffet ⁽¹⁴⁾)
100	5.6	5.1
200	11.3	10.1
300	16.9	15.2
400	22.5	20.3

(i) evaluation of the collision frequency.

The estimation of frequency is crucial in the argument flow. Our estimation is based on the kinetic of the ball movement⁽⁶⁾ that has been found to be oversimplified in comparison to the one appearing by direct *in situ* video recordings⁽⁸⁾⁽⁹⁾. Nevertheless, our values are in good agreement with those calculated (with an improved collision model) by Gaffet *et al.*⁽¹⁴⁾ as can be seen in Table 4. Further, other frequency values appeared in Ref. (9) do not differ substantially from those of the table.

(ii) Assumption of no reciprocal hindering

This point has been examined in Section II.2 where it has been shown that when n , is not so high (let us say one third⁽⁶⁾) the power measurements is directly proportional to the number of balls, that is the reciprocal hindering is really negligible.

In conclusion we fill that we have find out a fruitful

line of investigation in order to compare theory and experiment and along this line we are now pursuing our researches.

REFERENCES

- (1) J. S. Benjamin: Metall. Trans., **1** (1970), 2943.
- (2) P. S. Gilman and J. S. Benjamin: Ann. Rev. Mat. Sci. **5** (1983), 279.
- (3) R. B. Schwarz and C. C. Koch: Appl. Phys. Lett., **49** (1986), 146.
- (4) R. M. Davis, B. McDermott and C. C. Koch: Metall. Trans., **19A** (1988), 2867.
- (5) D. R. Maurice and T. H. Courtney: Metall. Trans., **21A** (1990), 289.
- (6) N. Burgio, A. Iasonna, M. Magini, S. Martelli and F. Padella: Nuovo Cimento, **13** (1991), 459.
- (7) F. Padella, E. Paradiso, N. Burgio, M. Magini, S. Martelli, W. Guo and A. Iasonna: J. Less Common Metals, **175** (1991), 79.
- (8) P. Le Brun, L. Froyen and L. Delaey: Mat. Sci. Eng., **A161** (1993), 75.
- (9) P. G. McCormick, H. Huang, M. P. Dallimore, J. Ding and J. Pan: *Mechanical Alloying for Structural Applications*, ed. by J. J. de Barbadillo, F. H. Froes and R. B. Schwarz, ASM., (1993), p. 45.
- (10) A. Iasonna, M. Magini and F. Padella: work in progress.
- (11) S. P. Timoshenko and J. N. Goodier: *Theory of Elasticity* McGraw-Hill, New York, (1970).
- (12) M. Magini, F. Padella, P. DeLogu, T. Dikonimos Makris and S. Turtù: Chem. Mat., **6** (1994), 983.
- (13) M. Magini, C. Colella, W. Guo, A. Iasonna, S. Martelli and F. Padella: J. Mechanochem. Mech. Alloying, **1** (1994), 14.
- (14) E. Gaffet, M. Abdellaoui and N. Malhouroux-Gaffet: Mater. Trans., JIM, **36** (1995), 198.